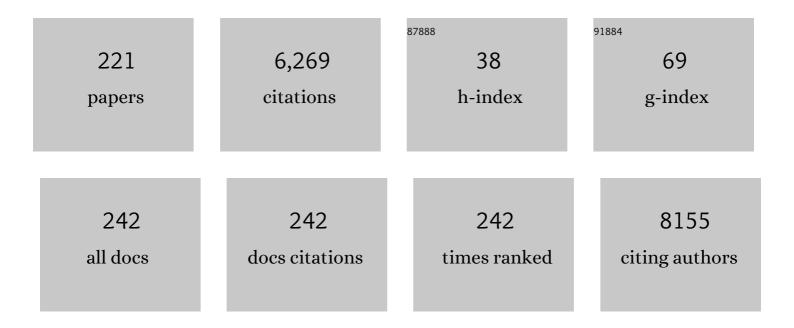
List of Publications by Year in descending order

Source: https://exaly.com/author-pdf/918847/publications.pdf Version: 2024-02-01



XIIMANC

#	Article	IF	CITATIONS
1	AHCYL1 senses SAH to inhibit autophagy through interaction with PIK3C3 in an MTORC1-independent manner. Autophagy, 2022, 18, 309-319.	9.1	17
2	Zonular defects in <i>loxl1</i> â€deficient zebrafish. Clinical and Experimental Ophthalmology, 2022, 50, 62-73.	2.6	2
3	Finite element stress analysis of the bearing component and bone resected surfaces for total ankle replacement with different implant material combinations. BMC Musculoskeletal Disorders, 2022, 23, 70.	1.9	4
4	Shape Approximation and Size Difference of the Upper Part of the Talus: Implication for Implant Design of the Talar Component for Total Ankle Replacement. BioMed Research International, 2022, 2022, 1-10.	1.9	3
5	Length change pattern of the ankle deltoid ligament during physiological ankle motion. Foot and Ankle Surgery, 2022, 28, 950-955.	1.7	1
6	Identification of Scd5 as a functional regulator of visceral fat deposition and distribution. IScience, 2022, 25, 103916.	4.1	3
7	Not Only in Sensorimotor Network: Local and Distant Cerebral Inherent Activity of Chronic Ankle Instability—A Resting-State fMRI Study. Frontiers in Neuroscience, 2022, 16, 835538.	2.8	6
8	Effect of loading history on material properties of human heel pad: an in-vivo pilot investigation during gait. BMC Musculoskeletal Disorders, 2022, 23, 254.	1.9	4
9	Effect of Purple Corn Anthocyanin on Antioxidant Activity, Volatile Compound and Sensory Property in Milk During Storage and Light Prevention. Frontiers in Nutrition, 2022, 9, 862689.	3.7	13
10	The effect of partial deltoid ligament injuries on the external rotation stability: A cadaveric study. Foot and Ankle Surgery, 2022, 28, 1215-1219.	1.7	1
11	Caveolinâ€1 promotes cancer progression via inhibiting ferroptosis in head and neck squamous cell carcinoma. Journal of Oral Pathology and Medicine, 2022, 51, 52-62.	2.7	36
12	Preoperative Lymphocyte-to-Monocyte Ratio Can Indicate the Outcomes in Repair of I-III Degree Injury of Lateral Ankle Ligament. BioMed Research International, 2022, 2022, 1-10.	1.9	1
13	Fabricating and Modulating Robust Multi-Photoaddressable Systems with the Derivatives of Diarylethylene and Donor–Acceptor Stenhouse Adducts. Journal of Physical Chemistry Letters, 2022, , 3611-3620.	4.6	1
14	Percutaneous Inferior Extensor Retinaculum Augmentation Technique for Chronic Ankle Instability. Orthopaedic Surgery, 2022, , .	1.8	1
15	Two-photon fluorescence imaging of the cerebral peroxynitrite stress in Alzheimer's disease. Chemical Communications, 2022, 58, 6300-6303.	4.1	25
16	Effects of Purple Corn Anthocyanin on Growth Performance, Meat Quality, Muscle Antioxidant Status, and Fatty Acid Profiles in Goats. Foods, 2022, 11, 1255.	4.3	16
17	CD73 in small extracellular vesicles derived from HNSCC defines tumourâ€associated immunosuppression mediated by macrophages in the microenvironment. Journal of Extracellular Vesicles, 2022, 11, e12218.	12.2	31
18	DDB1 prepares brown adipocytes for cold-induced thermogenesis. , 2022, 1, 39-53.		3

#	Article	IF	CITATIONS
19	Surgical management of concurrent lateral ankle instability and osteochondral lesions of the talus increases dynamic sagittal ankle range of motion. Knee Surgery, Sports Traumatology, Arthroscopy, 2022, 30, 3888-3897.	4.2	4
20	Heterogeneous UV disinfection aided by ZnO/Al ₂ O ₃ composites for inhibiting antibiotic resistant bacteria photoreactivation and gene recovery. Environmental Science: Nano, 2022, 9, 2488-2499.	4.3	3
21	The Effects of Selenium on Rumen Fermentation Parameters and Microbial Metagenome in Goats. Fermentation, 2022, 8, 240.	3.0	6
22	Photocontrollable Fluorescence Imaging of Mitochondrial Peroxynitrite during Ferroptosis with High Fidelity. Analytical Chemistry, 2022, 94, 10213-10220.	6.5	19
23	Nonstoichiometric tungsten oxide nanosheets with abundant oxygen vacancies for defectsâ€driven SERS sensing. Journal of Raman Spectroscopy, 2022, 53, 1880-1889.	2.5	3
24	Interactions between Escherichia coli survival and manganese and iron oxides in water under freeze-thaw. Environmental Pollution, 2021, 268, 115237.	7.5	1
25	Kdm6a suppresses the alternative activation of macrophages and impairs energy expenditure in obesity. Cell Death and Differentiation, 2021, 28, 1688-1704.	11.2	22
26	Midâ€ŧerm Results of Subtalar Arthroereisis with Talarâ€Fit Implant in Pediatric Flexible Flatfoot and Identifying the Effects of Adjunctive Procedures and Risk Factors for Sinus Tarsi Pain. Orthopaedic Surgery, 2021, 13, 175-184.	1.8	11
27	Influence of Achilles tendon rupture site on surgical repair outcomes. Journal of Orthopaedic Surgery, 2021, 29, 230949902110076.	1.0	4
28	The fibula and talus position difference in functional and mechanical ankle instability: MRI findings. Journal of Orthopaedic Surgery, 2021, 29, 230949902098457.	1.0	0
29	Acute exposure to N-Ethylpentylone induces developmental toxicity and dopaminergic receptor-regulated aberrances in zebrafish larvae. Toxicology and Applied Pharmacology, 2021, 417, 115477.	2.8	6
30	Multifunctional nanoplatforms as cascade-responsive drug-delivery carriers for effective synergistic chemo-photodynamic cancer treatment. Journal of Nanobiotechnology, 2021, 19, 140.	9.1	14
31	Systems Chemistry in Selfâ€Healing Materials. ChemSystemsChem, 2021, 3, e2100016.	2.6	6
32	Investigation on the contour and bone mineral density of the distal tibial cutting surface used for total ankle arthroplasty. Journal of Orthopaedic Surgery, 2021, 29, 230949902110280.	1.0	0
33	Targeting epigenetic modulation of cholesterol synthesis as a therapeutic strategy for head and neck squamous cell carcinoma. Cell Death and Disease, 2021, 12, 482.	6.3	13
34	An Investigation of Regional Plantar Soft Tissue Hardness and Its Potential Correlation with Plantar Pressure Distribution in Healthy Adults. Applied Bionics and Biomechanics, 2021, 2021, 1-9.	1.1	9
35	DDB1 binds histone reader BRWD3 to activate the transcriptional cascade in adipogenesis and promote onset of obesity. Cell Reports, 2021, 35, 109281.	6.4	9
36	Follicular Helper T Cells Remodel the Immune Microenvironment of Pancreatic Cancer via Secreting CXCL13 and IL-21. Cancers, 2021, 13, 3678.	3.7	37

#	Article	IF	CITATIONS
37	The Mediator subunit MED20 organizes the early adipogenic complex to promote development of adipose tissues and diet-induced obesity. Cell Reports, 2021, 36, 109314.	6.4	9
38	Targeting sorting nexin 10 improves mouse colitis via inhibiting PIKfyve-mediated TBK1/c-Rel signaling activation. Pharmacological Research, 2021, 169, 105679.	7.1	3
39	Biomechanical assessment of two types and two different locations of subtalar arthroereisis implants for flexible flatfoot: A cadaveric study. Clinical Biomechanics, 2021, 89, 105475.	1.2	3
40	Nuclear-targeted nanocarriers based on pH-sensitive amphiphiles for enhanced GNA002 delivery and chemotherapy. Nanoscale, 2021, 13, 4774-4784.	5.6	10
41	A near-infrared fluorogenic probe for nuclear thiophenol detection. Chemical Communications, 2021, 57, 2800-2803.	4.1	13
42	Manipulation of focal Wnt activity via synthetic cells in a doubleâ€humanized zebrafish model of tumorigenesis. International Journal of Cancer, 2021, 148, 2815-2824.	5.1	6
43	Knowledge atlas of post-traumatic epilepsy research: Based on citespace visualization analysis. Epilepsy Research, 2021, 178, 106790.	1.6	12
44	Combinatorial Normalization of Liver-Derived Cytokine Pathways Alleviates Hepatic Tumor-Associated Cachexia in Zebrafish. Cancer Research, 2021, 81, 873-884.	0.9	6
45	Harnessing Seî€N to develop novel fluorescent probes for visualizing the variation of endogenous hypobromous acid (HOBr) during the administration of an immunotherapeutic agent. Chemical Communications, 2021, 57, 12679-12682.	4.1	7
46	SNX10â€mediated LPS sensing causes intestinal barrier dysfunction via a caspaseâ€5â€dependent signaling cascade. EMBO Journal, 2021, 40, e108080.	7.8	22
47	Dual-Channel Imaging of Amyloid-β Plaques and Peroxynitrite To Illuminate Their Correlations in Alzheimer's Disease Using a Unimolecular Two-Photon Fluorescent Probe. Analytical Chemistry, 2021, 93, 15088-15095.	6.5	38
48	The neuropeptide calcitonin gene-related peptide links perineural invasion with lymph node metastasis in oral squamous cell carcinoma. BMC Cancer, 2021, 21, 1254.	2.6	8
49	Effect of Supplementation With Selenium-Yeast on Muscle Antioxidant Activity, Meat Quality, Fatty Acids and Amino Acids in Goats. Frontiers in Veterinary Science, 2021, 8, 813672.	2.2	20
50	Positive and negative factors for the treatment outcomes following total ankle arthroplasty? A systematic review. Foot and Ankle Surgery, 2020, 26, 1-13.	1.7	15
51	A polysaccharide from Grifola frondosa fruit body induces HT-29 cells apoptosis by PI3K/AKT-MAPKs and NF-κB-pathway. International Journal of Biological Macromolecules, 2020, 147, 79-88.	7.5	26
52	An overlap of antineutrophil cytoplasmic antibody (ANCA)-associated glomerulonephritis and IgG4-related kidney disease. Clinica Chimica Acta, 2020, 501, 12-19.	1.1	6
53	Stair descent biomechanics reflect perceived instability in people with unilateral ankle sprain history. Clinical Biomechanics, 2020, 72, 52-57.	1.2	6
54	LASP1 promotes proliferation, metastasis, invasion in head and neck squamous cell carcinoma and through direct interaction with HSPA1A. Journal of Cellular and Molecular Medicine, 2020, 24, 1626-1639.	3.6	16

#	Article	IF	CITATIONS
55	Design and validation of a foot–ankle dynamic simulator with a 6-degree-of-freedom parallel mechanism. Proceedings of the Institution of Mechanical Engineers, Part H: Journal of Engineering in Medicine, 2020, 234, 1070-1082.	1.8	4
56	Finite element analysis of the initial stability of arthroscopic ankle arthrodesis with three-screw fixation: posteromedial versus posterolateral home-run screw. Journal of Orthopaedic Surgery and Research, 2020, 15, 252.	2.3	5
57	Influence of high-heeled shoe parameters on biomechanical performance of young female adults during stair ascent motion. Gait and Posture, 2020, 81, 159-165.	1.4	2
58	A Retrospective Study on the Morphology of Posterior Malleolar Fractures Based on a CT Scan: Whether We Ignore the Importance of Fracture Height. BioMed Research International, 2020, 2020, 1-8.	1.9	4
59	In vitro study of foot bone kinematics via a custom-made cadaveric gait simulator. Journal of Orthopaedic Surgery and Research, 2020, 15, 346.	2.3	6
60	Finite-element analysis of the influence of tibial implant fixation design of total ankle replacement on bone–implant interfacial biomechanical performance. Journal of Orthopaedic Surgery, 2020, 28, 230949902096612.	1.0	10
61	Sorting Nexin 10 Mediates Metabolic Reprogramming of Macrophages in Atherosclerosis Through the Lyn-Dependent TFEB Signaling Pathway. Circulation Research, 2020, 127, 534-549.	4.5	32
62	BIG1 controls macrophage pro-inflammatory responses through ARF3-mediated PI(4,5)P2 synthesis. Cell Death and Disease, 2020, 11, 374.	6.3	12
63	Immunomodulatory effects of the polysaccharide from Craterellus cornucopioides via activating the TLR4-NFI°B signaling pathway in peritoneal macrophages of BALB/c mice. International Journal of Biological Macromolecules, 2020, 160, 871-879.	7.5	13
64	Zoledronic acid regulates the synthesis and secretion of IL- $1^{\hat{l}2}$ through Histone methylation in macrophages. Cell Death Discovery, 2020, 6, 47.	4.7	15
65	High homocysteine promotes telomere dysfunction and chromosomal instability in human neuroblastoma SH-SY5Y cells. Mutation Research - Genetic Toxicology and Environmental Mutagenesis, 2020, 854-855, 503197.	1.7	5
66	A Radiographic Study of Biomechanical Relationship between the Achilles Tendon and Plantar Fascia. BioMed Research International, 2020, 2020, 1-6.	1.9	4
67	Risk factors for metastasis and poor prognosis of Ewing sarcoma: a population based study. Journal of Orthopaedic Surgery and Research, 2020, 15, 88.	2.3	26
68	Long noncoding RNA <i>KTN1-AS1</i> promotes head and neck squamous cell carcinoma cell epithelial–mesenchymal transition by targeting <i>miR-153-3p</i> . Epigenomics, 2020, 12, 487-505.	2.1	25
69	Identification of MicroRNA–Potassium Channel Messenger RNA Interactions in the Brain of Rats With Post-traumatic Epilepsy. Frontiers in Molecular Neuroscience, 2020, 13, 610090.	2.9	3
70	Modeling of Solid-Tumor Microenvironment in Zebrafish (Danio Rerio) Larvae. Advances in Experimental Medicine and Biology, 2020, 1219, 413-428.	1.6	10
71	Calcitonin gene-related peptide: A promising bridge between cancer development and cancer-associated pain in oral squamous cell carcinoma. Oncology Letters, 2020, 20, 253.	1.8	3
72	Calcitonin gene‑related peptide: A promising bridge between cancer development and cancer‑associated pain in oral squamous cell carcinoma (Review). Oncology Letters, 2020, 20, 1-1.	1.8	12

#	Article	IF	CITATIONS
73	In vivo kinematics of functional ankle instability patients during the stance phase of walking. Gait and Posture, 2019, 73, 262-268.	1.4	19
74	Transgenic strategies to generate heterogeneous hepatic cancer models in zebrafish. Journal of Molecular Cell Biology, 2019, 11, 1021-1023.	3.3	4
75	LncRNA LINC00460 promotes EMT in head and neck squamous cell carcinoma by facilitating peroxiredoxin-1 into the nucleus. Journal of Experimental and Clinical Cancer Research, 2019, 38, 365.	8.6	117
76	Discovery of a virus of the species Enterovirus F in goats. Archives of Virology, 2019, 164, 2551-2558.	2.1	5
77	Identification of three linear B cell epitopes using monoclonal antibodies against bovine enterovirus VP2 protein. Applied Microbiology and Biotechnology, 2019, 103, 7467-7480.	3.6	5
78	Effects of an ankle brace on the in vivo kinematics of patients with chronic ankle instability during walking on an inversion platform. Gait and Posture, 2019, 72, 228-233.	1.4	10
79	Novel TRRAP mutation causes autosomal dominant nonâ€syndromic hearing loss. Clinical Genetics, 2019, 96, 300-308.	2.0	11
80	Patient-derived Heterogeneous Xenograft Model of Pancreatic Cancer Using Zebrafish Larvae as Hosts for Comparative Drug Assessment. Journal of Visualized Experiments, 2019, , .	0.3	11
81	A Facile, Versatile, and Highly Efficient Strategy for Peroxynitrite Bioimaging Enabled by Formamide Deformylation. Analytical Chemistry, 2019, 91, 6872-6879.	6.5	32
82	Effect of a Semirigid Ankle Brace on the In Vivo Kinematics of Patients with Functional Ankle Instability during the Stance Phase of Walking. BioMed Research International, 2019, 2019, 1-10.	1.9	3
83	Dynamic Coordinated Active–Reactive Power Optimization for Active Distribution Network with Energy Storage Systems. Applied Sciences (Switzerland), 2019, 9, 1129.	2.5	8
84	Reliability and validity of different ankle MRI scanning planes for the anterior talofibular ligament injury diagnosis: a cadaveric study. Journal of Orthopaedic Surgery and Research, 2019, 14, 69.	2.3	4
85	ldentification of a 42â€bp heartâ€specific enhancer of the <i>notch1b</i> gene in zebrafish embryos. Developmental Dynamics, 2019, 248, 426-436.	1.8	5
86	In Vivo Kinematics of Functional Ankle Instability Patients and Lateral Ankle Sprain Copers During Stair Descent. Journal of Orthopaedic Research, 2019, 37, 1860-1867.	2.3	13
87	Reactivity Modulation of Benzopyran-Coumarin Platform by Introducing Electron-Withdrawing Groups: Specific Detection of Biothiols and Peroxynitrite. Analytical Chemistry, 2019, 91, 6097-6102.	6.5	22
88	Derotation of the Talus and Arthrodesis Treatment of Stages II-V Müller-Weiss Disease: Midterm Results of 36 Cases. Foot and Ankle International, 2019, 40, 506-514.	2.3	8
89	Leptin induces muscle wasting in <i>kras</i> -driven hepatocellular carcinoma (HCC) model in zebrafish. DMM Disease Models and Mechanisms, 2019, 12, .	2.4	21
90	Discovery and Profiling of microRNAs at the Critical Period of Sex Differentiation in Xanthoceras sorbifolium Bunge. Forests, 2019, 10, 1141.	2.1	10

#	Article	IF	CITATIONS
91	Combinatorial genetic replenishments in myocardial and outflow tract tissues restore heart function in <i>tnnt2</i> mutant zebrafish. Biology Open, 2019, 8, .	1.2	7
92	Impact of first metatarsal shortening on forefoot loading pattern: a finite element model study. BMC Musculoskeletal Disorders, 2019, 20, 625.	1.9	20
93	EFTUD2 gene deficiency disrupts osteoblast maturation and inhibits chondrocyte differentiation via activation of the p53 signaling pathway. Human Genomics, 2019, 13, 63.	2.9	17
94	Outcome Comparison Between Functional Ankle Instability Cases With and Without Anterior Ankle Impingement: A Retrospective Cohort Study. Journal of Foot and Ankle Surgery, 2019, 58, 52-56.	1.0	8
95	Exosomal miR-196a derived from cancer-associated fibroblasts confers cisplatin resistance in head and neck cancer through targeting CDKN1B and ING5. Genome Biology, 2019, 20, 12.	8.8	291
96	Pathological kinematic patterns of the tarsal complex in stage II adultâ€acquired flatfoot deformity. Journal of Orthopaedic Research, 2019, 37, 477-482.	2.3	6
97	A hint from zebrafish models of hepatic tumorigenesis: Targeting stearoyl-CoA desaturase. Oncotarget, 2019, 10, 924-925.	1.8	3
98	Immunomodulatory Activity of Docosahexenoic Acid on RAW264.7 Cells Activation through GPR120-Mediated Signaling Pathway. Journal of Agricultural and Food Chemistry, 2018, 66, 926-934.	5.2	33
99	Csy4-based vector system enables conditional chimeric gene editing in zebrafish without interrupting embryogenesis. Journal of Molecular Cell Biology, 2018, 10, 586-588.	3.3	9
100	Recent advances in vitamins analysis by capillary electrophoresis. Journal of Pharmaceutical and Biomedical Analysis, 2018, 147, 278-287.	2.8	38
101	Preparation, characterization and calcium release evaluation in vitro of casein phosphopeptides-soluble dietary fibers copolymers as calcium delivery system. Food Chemistry, 2018, 245, 262-269.	8.2	26
102	Small-Molecule Fluorescent Probes for Imaging and Detection of Reactive Oxygen, Nitrogen, and Sulfur Species in Biological Systems. Analytical Chemistry, 2018, 90, 533-555.	6.5	412
103	Morphological variation, genetic differentiation and phylogeography of the <scp>E</scp> ast <scp>A</scp> sia cicada <i>Hyalessa maculaticollis</i> (<scp>H</scp> emiptera: <scp>C</scp> icadidae). Systematic Entomology, 2018, 43, 308-329.	3.9	22
104	A two-photon fluorescent probe for ratiometric visualization of hypochlorous acid in live cells and animals based on a selenide oxidation/elimination tandem reaction. Chemical Communications, 2018, 54, 11965-11968.	4.1	66
105	A 20(S)‑protopanaxadiol derivative PPD12 reverses ABCB1‑mediated multidrug resistance with oral bioavailability and low toxicity. Oncology Letters, 2018, 16, 5891-5899.	1.8	2
106	Metallic hollow waveguide based on GeO2–NaOH precursor solution for transmission of CO2 laser radiations. Optical and Quantum Electronics, 2018, 50, 1.	3.3	3
107	Selective and sensitive determination of tetracyclines by HPLC with chemiluminescence detection based on a cerium(IV)â€methoxylated cypridina luciferin analogue system. Journal of Separation Science, 2018, 41, 4115-4121.	2.5	11
108	<i>Paradiplozoon yunnanensis</i> n. sp. (Monogenea, Diplozoidae) from <i>Sikukia gudgeri</i> (Cyprinidae, Barbinae) in southwest China. Parasite, 2018, 25, 46.	2.0	7

#	Article	IF	CITATIONS
109	Mitochondrial Peroxynitrite Mediation of Anthracycline-Induced Cardiotoxicity as Visualized by a Two-Photon Near-Infrared Fluorescent Probe. Analytical Chemistry, 2018, 90, 11629-11635.	6.5	105
110	Evaluating Drug-Induced Liver Injury and Its Remission via Discrimination and Imaging of HClO and H ₂ S with a Two-Photon Fluorescent Probe. Analytical Chemistry, 2018, 90, 7510-7516.	6.5	98
111	Canonical Wnt Signaling Remodels Lipid Metabolism in Zebrafish Hepatocytes following Ras Oncogenic Insult. Cancer Research, 2018, 78, 5548-5560.	0.9	47
112	A Twoâ€Photon H ₂ O ₂ â€Activated CO Photoreleaser. Angewandte Chemie, 2018, 130, 12595-12599.	2.0	12
113	Cancer-associated Fibroblast-derived IL-6 Promotes Head and Neck Cancer Progression via the Osteopontin-NF-kappa B Signaling Pathway. Theranostics, 2018, 8, 921-940.	10.0	128
114	A Twoâ€Photon H ₂ O ₂ â€Activated CO Photoreleaser. Angewandte Chemie - International Edition, 2018, 57, 12415-12419.	13.8	80
115	Imaging diagnosis for chronic lateral ankle ligament injury: a systemic review with meta-analysis. Journal of Orthopaedic Surgery and Research, 2018, 13, 122.	2.3	56
116	Thermal oxidation-resistant GeO2 ATR hollow waveguide based on NiCr capillary tube and its thermal effects. Applied Physics B: Lasers and Optics, 2018, 124, 1.	2.2	0
117	Modelling of the ICF core sets for chronic ischemic heart disease using the LASSO model in Chinese patients. Health and Quality of Life Outcomes, 2018, 16, 139.	2.4	6
118	Arthrodesis for Treatment of Intra-Articular Synovial Cysts of the Hallux Interphalangeal Joint. Journal of Foot and Ankle Surgery, 2018, 57, 1221-1224.	1.0	4
119	Gender Variation in the Shape of Superior Talar Dome: A Cadaver Measurement Based on Chinese Population. BioMed Research International, 2018, 2018, 1-7.	1.9	4
120	Shelterin differentially respond to oxidative stress induced by TiO2-NPs and regulate telomere length in human hepatocytes andÂhepatocarcinoma cells inÂvitro. Biochemical and Biophysical Research Communications, 2018, 503, 697-702.	2.1	11
121	Recent Advances in Nutrition for the Treatment of Depressive Disorder. Current Pharmaceutical Design, 2018, 24, 2583-2590.	1.9	7
122	A three-IncRNA signature derived from the Atlas of ncRNA in cancer (TANRIC) database predicts the survival of patients with head and neck squamous cell carcinoma. Oral Oncology, 2017, 65, 94-101.	1.5	134
123	Comparison of Four Methods for Percutaneous Achilles Tendon Lengthening: A Cadaveric Study. Journal of Foot and Ankle Surgery, 2017, 56, 271-276.	1.0	8
124	Combinatorial Strategy to Identify Fluorescent Probes for Biothiol and Thiophenol Based on Diversified Pyrimidine Moieties and Their Biological Applications. Analytical Chemistry, 2017, 89, 3015-3020.	6.5	63
125	Preparation of cucumber seed peptide-calcium chelate by liquid state fermentation and its characterization. Food Chemistry, 2017, 229, 487-494.	8.2	94
126	Association between the MTHFR C677T polymorphism, blood folate and vitamin B12 deficiency, and elevated serum total homocysteine in healthy individuals in Yunnan Province, China. Journal of the Chinese Medical Association, 2017, 80, 147-153.	1.4	46

#	Article	IF	CITATIONS
127	Simultaneous Fluorescence and Chemiluminescence Turned on by Aggregation-Induced Emission for Real-Time Monitoring of Endogenous Superoxide Anion in Live Cells. Analytical Chemistry, 2017, 89, 7210-7215.	6.5	80
128	Acetylation of Cavin-1 Promotes Lipolysis in White Adipose Tissue. Molecular and Cellular Biology, 2017, 37, .	2.3	10
129	Dietary Antioxidants: Potential Anticancer Agents. Nutrition and Cancer, 2017, 69, 521-533.	2.0	45
130	A covalently bound inhibitor triggers <scp>EZH</scp> 2 degradation through <scp>CHIP</scp> â€mediated ubiquitination. EMBO Journal, 2017, 36, 1243-1260.	7.8	67
131	Sleep disorders and allergic diseases in Chinese toddlers. Sleep Medicine, 2017, 37, 174-179.	1.6	21
132	Treatment of Medial Malleolus or Pure Deltoid Ligament Injury in Patients with Supinationâ€External Rotation Type <scp>IV</scp> Ankle Fractures. Orthopaedic Surgery, 2017, 9, 42-48.	1.8	15
133	Two-photon fluorescent probe for revealing drug-induced hepatotoxicity via mapping fluctuation of peroxynitrite. Chemical Science, 2017, 8, 4006-4011.	7.4	171
134	Disruption of the <i>gaa</i> Gene in Zebrafish Fails to Generate the Phenotype of Classical Pompe Disease. DNA and Cell Biology, 2017, 36, 10-17.	1.9	7
135	Twin Derivatization Strategy for High-Coverage Quantification of Free Fatty Acids by Liquid Chromatography–Tandem Mass Spectrometry. Analytical Chemistry, 2017, 89, 12223-12230.	6.5	72
136	New role of LRP5, associated with nonsyndromic autosomal-recessive hereditary hearing loss. Human Mutation, 2017, 38, 1421-1431.	2.5	8
137	High Resolution Imaging of DNA Methylation Dynamics using a Zebrafish Reporter. Scientific Reports, 2017, 7, 5430.	3.3	10
138	Screening in larval zebrafish reveals tissue-specific distributions of fifteen fluorescent compounds. DMM Disease Models and Mechanisms, 2017, 10, 1155-1164.	2.4	19
139	Biomechanical Study of Screw Fixation and Plate Fixation of a Posterior Malleolar Fracture in a Simulation of the Normal Gait Cycle. Foot and Ankle International, 2017, 38, 1132-1138.	2.3	18
140	Study on light-capture performance of silicon thin-film hollow waveguide solar cells. Optical and Quantum Electronics, 2017, 49, 1.	3.3	1
141	Sustentacular screw placement with guidance during ORIF of calcaneal fracture: an anatomical specimen study. Journal of Orthopaedic Surgery and Research, 2017, 12, 78.	2.3	14
142	Dual-phase stimulated Raman scattering microscopy for real-time two-color imaging. Optica, 2017, 4, 44.	9.3	86
143	Casein Glycomacropeptide Hydrolysates Exert Cytoprotective Effect against Cellular Oxidative Stress by Up-Regulating HO-1 Expression in HepG2 Cells. Nutrients, 2017, 9, 31.	4.1	23
144	The Transcription Factor Bach1 Suppresses the Developmental Angiogenesis of Zebrafish. Oxidative Medicine and Cellular Longevity, 2017, 2017, 1-10.	4.0	25

#	Article	IF	CITATIONS
145	Loading pattern of postoperative hallux valgus feet with and without transfer metatarsalgia: a case control study. Journal of Orthopaedic Surgery and Research, 2017, 12, 120.	2.3	9
146	Maternal Urinary Triclosan Concentration in Relation to Maternal and Neonatal Thyroid Hormone Levels: A Prospective Study. Environmental Health Perspectives, 2017, 125, 067017.	6.0	76
147	Response of MiRNA-22-3p and MiRNA-149-5p to Folate Deficiency and the Differential Regulation of MTHFR Expression in Normal and Cancerous Human Hepatocytes. PLoS ONE, 2017, 12, e0168049.	2.5	13
148	Effect of JNK inhibitor SP600125 on hair cell regeneration in zebrafish (<i>Danio rerio</i>) larvae. Oncotarget, 2016, 7, 51640-51650.	1.8	33
149	The Role of Genetic Polymorphisms as Related to One-Carbon Metabolism, Vitamin B6, and Gene–Nutrient Interactions in Maintaining Genomic Stability and Cell Viability in Chinese Breast Cancer Patients. International Journal of Molecular Sciences, 2016, 17, 1003.	4.1	10
150	Accurate determination of screw position in treating fifth metatarsal base fractures to shorten radiation exposure time. Singapore Medical Journal, 2016, 57, 619-623.	0.6	3
151	Complications of Ankle Fusion for Treating Late Sequelae of Ankle Injuries. Journal of Hard Tissue Biology, 2016, 25, 165-172.	0.4	1
152	SLC44A4mutation causes autosomal dominant hereditary postlingual non-syndromic mid-frequency hearing loss. Human Molecular Genetics, 2016, 26, ddw394.	2.9	9
153	TGFβ3-mediated induction of Periostin facilitates head and neck cancer growth and is associated with metastasis. Scientific Reports, 2016, 6, 20587.	3.3	84
154	In vivo kinematic study of the tarsal joints complex based on fluoroscopic 3D-2D registration technique. Gait and Posture, 2016, 49, 54-60.	1.4	20
155	Multicolor Fluorescence Detection-Based Microfluidic Device for Single-Cell Metabolomics: Simultaneous Quantitation of Multiple Small Molecules in Primary Liver Cells. Analytical Chemistry, 2016, 88, 8610-8616.	6.5	62
156	A new species of the genus Hyalessa (Hemiptera, Cicadidae) from China,Âwith DNA barcoding data and a key to related species. Zootaxa, 2016, 4085, 296-300.	0.5	2
157	Role of Sirtuins in Maintenance of Genomic Stability: Relevance to Cancer and Healthy Aging. DNA and Cell Biology, 2016, 35, 542-575.	1.9	25
158	Rational Design of an α-Ketoamide-Based Near-Infrared Fluorescent Probe Specific for Hydrogen Peroxide in Living Systems. Analytical Chemistry, 2016, 88, 8019-8025.	6.5	139
159	A systematic evaluation for the potential translation of CD166-related expression as a cancer biomarker. Expert Review of Molecular Diagnostics, 2016, 16, 925-932.	3.1	10
160	Fluorescent Probe Based on Azobenzene-Cyclopalladium for the Selective Imaging of Endogenous Carbon Monoxide under Hypoxia Conditions. Analytical Chemistry, 2016, 88, 11154-11159.	6.5	112
161	Neighborhood Disadvantage, Poor Social Conditions, and Cardiovascular Disease Incidence Among African American Adults in the Jackson Heart Study. American Journal of Public Health, 2016, 106, 2219-2226.	2.7	102
162	Applications and challenges for single-bacteria analysis by flow cytometry. Science China Chemistry, 2016, 59, 30-39.	8.2	36

#	Article	IF	CITATIONS
163	The impact of high-heeled shoes on ankle complex during walking in young women—In vivo kinematic study based on 3D to 2D registration technique. Journal of Electromyography and Kinesiology, 2016, 28, 7-16.	1.7	18
164	Lateral Sesamoid Position Relative to the Second Metatarsal in Feet With and Without Hallux Valgus: A Prospective Study. Journal of Foot and Ankle Surgery, 2016, 55, 136-139.	1.0	20
165	Preparation of graphene/TiO ₂ nanotube array photoelectrodes and their photocatalytic activity for the degradation of alachlor. Catalysis Science and Technology, 2016, 6, 1892-1902.	4.1	23
166	Osteochondroma of the Talar Neck: A Case Report and Literature Review. Journal of Foot and Ankle Surgery, 2016, 55, 338-344.	1.0	10
167	CD73 is associated with poor prognosis in HNSCC. Oncotarget, 2016, 7, 61690-61702.	1.8	57
168	X-linked FHL1 as a novel therapeutic target for head and neck squamous cell carcinoma. Oncotarget, 2016, 7, 14537-14550.	1.8	11
169	A review of the cicada genus Haphsa Distant from China (Hemiptera: Cicadidae). Zootaxa, 2015, 3957, 408.	0.5	0
170	Mobility of the first metatarsal-cuneiform joint in patients with and without hallux valgus: in vivo three-dimensional analysis using computerized tomography scan. Journal of Orthopaedic Surgery and Research, 2015, 10, 140.	2.3	56
171	Long-term antiviral efficacy of entecavir and liver histology improvement in Chinese patients with hepatitis B virus-related cirrhosis. World Journal of Gastroenterology, 2015, 21, 7869.	3.3	23
172	Anatomy of the Sural Nerve With an Emphasis on the Incision for Medial Displacement Calcaneal Osteotomy. Journal of Foot and Ankle Surgery, 2015, 54, 341-344.	1.0	14
173	U0126 inhibits pancreatic cancer progression via the KRAS signaling pathway in a zebrafish xenotransplantation model. Oncology Reports, 2015, 34, 699-706.	2.6	26
174	Bach1 Represses Wnt/ \hat{l}^2 -Catenin Signaling and Angiogenesis. Circulation Research, 2015, 117, 364-375.	4.5	113
175	Kinetics of BTEX biodegradation coupled with Fe(III) reduction by indigenous microorganisms in simulated underground environment. Desalination and Water Treatment, 2015, 54, 2334-2341.	1.0	4
176	Dual-calibration coefficient: a more accurate protocol for simultaneous determination of superoxide and hydrogen peroxide in human HepG2 cell extracts. Science China Chemistry, 2015, 58, 825-829.	8.2	5
177	Three-dimensional motions of distal syndesmosis during walking. Journal of Orthopaedic Surgery and Research, 2015, 10, 166.	2.3	17
178	A single-beam-splitting technique combined with a calibration-free method for field-deployable applications using laser-induced breakdown spectroscopy. RSC Advances, 2015, 5, 4537-4546.	3.6	14
179	Comparison of Wedge Resection (Winograd Procedure) and Wedge Resection Plus Complete Nail Plate Avulsion in the Treatment of Ingrown Toenails. Journal of Foot and Ankle Surgery, 2015, 54, 395-398.	1.0	20
180	Rehabilitation Regimen After Surgical Treatment of Acute Achilles Tendon Ruptures. American Journal of Sports Medicine, 2015, 43, 1008-1016.	4.2	88

#	Article	IF	CITATIONS
181	Botulinum Toxin Type A Injection Combined With Cast Immobilization for Treating Recurrent Peroneal Spastic Flatfoot Without Bone Coalitions: A Case Report and Review of the Literature. Journal of Foot and Ankle Surgery, 2015, 54, 697-700.	1.0	5
182	Different Sutures in the Surgical Treatment of Acute Closed Achilles Tendon Rupture. Indian Journal of Surgery, 2015, 77, 936-940.	0.3	5
183	Solute Carrier Family 26 Member a2 (slc26a2) Regulates Otic Development and Hair Cell Survival in Zebrafish. PLoS ONE, 2015, 10, e0136832.	2.5	6
184	Beneficial effects of cannabinoid receptor type 2 (CB2R) in injured skeletal muscle post-contusion. Histology and Histopathology, 2015, 30, 737-49.	0.7	8
185	Bezoar-induced small bowel obstruction: Clinical characteristics and diagnostic value of multi-slice spiral computed tomography. World Journal of Gastroenterology, 2015, 21, 9774.	3.3	39
186	The clinical translational potential of p53-related alterations as cancer biomarkers. Histology and Histopathology, 2015, 30, 1171-83.	0.7	4
187	On cicadas of Hyalessa maculaticollis complex (Hemiptera, Cicadidae) of China. ZooKeys, 2014, 369, 25-41.	1.1	9
188	Treatment of Chronic Deltoid Ligament Injury Using Suture Anchors. Orthopaedic Surgery, 2014, 6, 223-228.	1.8	6
189	Screening and investigation of a cyanine fluorescent probe for simultaneous sensing of glutathione and cysteine under single excitation. Chemical Communications, 2014, 50, 15439-15442.	4.1	113
190	Ildr1b is essential for semicircular canal development, migration of the posterior lateral line primordium and hearing ability in zebrafish: implications for a role in the recessive hearing impairment DFNB42. Human Molecular Genetics, 2014, 23, 6201-6211.	2.9	16
191	Plasma homocysteine levels and genetic polymorphisms in folate metablism are associated with breast cancer risk in chinese women. Hereditary Cancer in Clinical Practice, 2014, 12, 2.	1.5	35
192	Review of the cicada genus Platylomia Stål (Hemiptera, Cicadidae) from China, with description and bioacoustics of a new species from Mts. Qinling . Zootaxa, 2014, 3811, 137.	0.5	3
193	Regulatory effect and mechanisms of carbon monoxide-releasing molecule II on hepatic energy metabolism in septic mice. World Journal of Gastroenterology, 2014, 20, 3301.	3.3	4
194	A reappraisal of the relationship between metatarsus adductus and hallux valgus. Chinese Medical Journal, 2014, 127, 2067-72.	2.3	3
195	Selective recognition of beta ypermethrin by molecularly imprinted polymers based on magnetite yeast composites. Journal of Applied Polymer Science, 2013, 129, 1952-1958.	2.6	8
196	Gambogic Acid as a Nonâ€Competitive Inhibitor of ATPâ€Binding Cassette Transporter B1 Reverses the Multidrug Resistance of Human Epithelial Cancers by Promoting ATPâ€Binding Cassette Transporter B1 Protein Degradation. Basic and Clinical Pharmacology and Toxicology, 2013, 112, 25-33.	2.5	41
197	A near-infrared ratiometric fluorescent probe for rapid and highly sensitive imaging of endogenous hydrogen sulfide in living cells. Chemical Science, 2013, 4, 2551.	7.4	319
198	Anatomical factors affecting the selection of an operative approach for fibular fractures involving the posterior malleolus. Experimental and Therapeutic Medicine, 2013, 5, 757-760.	1.8	4

#	Article	IF	CITATIONS
199	Gambogic Acid is a Novel Anti-cancer Agent that Inhibits Cell Proliferation, Angiogenesis and Metastasis. Anti-Cancer Agents in Medicinal Chemistry, 2012, 12, 994-1000.	1.7	77
200	Photoinduced charge separation enhanced by the confinement of electron donor and acceptor at different surfaces of porous TiO2 nanotubes and its application in olefin oxidation. Journal of Materials Chemistry, 2012, 22, 11915.	6.7	6
201	Wnt Signaling Regulates Postembryonic Hypothalamic Progenitor Differentiation. Developmental Cell, 2012, 23, 624-636.	7.0	90
202	Flatfoot in Müller-Weiss syndrome: a case series. Journal of Medical Case Reports, 2012, 6, 228.	0.8	19
203	Effect of additive triblock copolymer PEP-3100 on bottom-up filling in electroless copper plating. Russian Journal of Electrochemistry, 2012, 48, 99-103.	0.9	2
204	Dualâ€Luminophoreâ€Labeled Gold Nanoparticles with Completely Resolved Emission for the Simultaneous Imaging of MMPâ€2 and MMPâ€7 in Living Cells under Single Wavelength Excitation. Chemistry - A European Journal, 2012, 18, 7189-7195.	3.3	30
205	Ankle fusion with a retrograde locked intramedullary nail for sequela of lower extremity compartment syndrome. Chinese Journal of Traumatology - English Edition, 2012, 15, 140-4.	1.4	2
206	Preparation and characteristics of yak casein hydrolysate–iron complex. International Journal of Food Science and Technology, 2011, 46, 1705-1710.	2.7	39
207	Progenitor expansion in apc mutants is mediated by Jak/Stat signaling. BMC Developmental Biology, 2011, 11, 73.	2.1	13
208	Classification and identification of damage mechanisms in polyethylene selfâ€reinforced laminates by acoustic emission technique. Polymer Composites, 2011, 32, 945-959.	4.6	17
209	Comparison of Bottom-up Filling in Electroless Plating with an Addition of PEG, PPG and EPE. Chinese Journal of Chemistry, 2011, 29, 422-426.	4.9	5
210	Genome-Wide Linkage Scan of a Pedigree with Familial Hypercholesterolemia Suggests Susceptibility Loci on Chromosomes 3q25-26 and 21q22. PLoS ONE, 2011, 6, e24838.	2.5	12
211	Mechanical behaviors of the foot after individual releases of plantar fascia and ligaments during the balanced standing. Journal of Shanghai Jiaotong University (Science), 2010, 15, 726-729.	0.9	2
212	Identification of Wnt-Responsive Cells in the Zebrafish Hypothalamus. Zebrafish, 2009, 6, 49-58.	1.1	36
213	Tcf3 inhibits spinal cord neurogenesis by regulating <i>sox4a</i> expression. Development (Cambridge), 2009, 136, 781-789.	2.5	36
214	An In Vivo Experimental Validation of a Computational Model of Human Foot. Journal of Bionic Engineering, 2009, 6, 387-397.	5.0	58
215	Hierarchical assembly of CdTe nanotubes and nanowires at water–oil interface. Journal of Materials Chemistry, 2009, 19, 3027.	6.7	14
216	Management of the Second and Third Metatarsal in Moderate and Severe Hallux Valgus. Orthopedics, 2009. 32. 892.	1.1	11

#	Article	IF	CITATIONS
217	A comparison of folic acid deficiency-induced genomic instability in lymphocytes of breast cancer patients and normal non-cancer controls from a Chinese population in Yunnan. Mutagenesis, 2006, 21, 41-47.	2.6	20
218	Folate deficiency induces aneuploidy in human lymphocytes in vitro—evidence using cytokinesis-blocked cells and probes specific for chromosomes 17 and 21. Mutation Research - Fundamental and Molecular Mechanisms of Mutagenesis, 2004, 551, 167-180.	1.0	107
219	Optimized HY via Thermal Modification as a Green Catalyst for One-Pot Synthesis of Fructose from Glucose Isomerization in Methanol/Water Medium. Catalysis Letters, 0, , 1.	2.6	Ο
220	Neoadjuvant chemotherapy endows <scp>CD9</scp> with prognostic value that differs between tumor and stromal areas in patients with pancreatic cancer. Journal of Clinical Laboratory Analysis, 0, , .	2.1	3
221	Epidemiological Characteristics of Patients Operated for Achilles Tendon Rupture in Shanghai. Orthopaedic Surgery, 0, , .	1.8	1